RAMAN SCATTERING STUDY OF $(Sr,Ca)_{10}Cu_{17}O_{29}$ SINGLE CRYSTALS

J. STRZESZEWSKI[a,*], H. SZYMCZAK[b], L. LEONYUK[c] AND R. SZYMCZAK[b]

[a]Faculty of Physics, Warsaw University of Technology
Koszykowa 75, 00-661 Warsaw, Poland
[b]Institute of Physics, Polish Academy of Sciences
Al. Lotników 32/46, 02-668 Warsaw, Poland
[c]Geological Department, Moscow State University, 119899 Moscow, Russia

(Received September 4, 2000)

Polarized Raman spectra of high temperature superconducting single crystals of $A_{10}Cu_{17}O_{29}$ ($A_{10} = Ca_{4.7}Sr_{4.1}Bi_{0.3}$) were studied in various scattering configurations in the range of 40–700 cm^{-1}. In very distinctive spectra there were found over 20 peaks. It was observed that the flat continuum of electronic excitations in the normal state was redistributed below the critical temperature. The frequency dependent redistribution is consistent with the value of energy gap estimated using tunnelling spectroscopy techniques.

PACS numbers: 78.30.Hv, 74.25.Gz, 74.25.-q

1. Introduction

The orthorhombic compound $A_{10}Cu_{17}O_{29}$ (where A are alkaline earth and/or trivalent metals) belongs to the spin ladder compounds consisting of two structural modules: $A_2Cu_2O_3$ and CuO_2 with characteristic of them Cu_2O_3 two-leg ladder layers and CuO_2 one-dimensional chains [1–4]. Both modules have identical a and b lattice constants and different incommensurate c parameters. The compound $A_{10}Cu_{17}O_{29}$ is a member of larger family $(A_2Cu_2O_3)_m(CuO_2)_n$ with $m/n = 5/7$, $7/10$, and $9/13$ [4]. Recently, the superconductivity observations in this compound have been reported with the critical temperature of about 80 K [5, 6]. Superconductivity under pressure was also found in 7/10 compound [7]. It should be emphasized that for the first time the superconductivity occurs rather in Cu_2O_3 layers than in CuO_2 layers, as it is for other high-T_c superconductors.

Raman scattering has been widely used to study the high-T_c superconductors (see review papers [8] and [9] on Raman scattering in cuprate superconductors). So far there are only few reports on Raman measurements for spin ladder 7/10 systems

*corresponding author, e-mail: strze@if.pw.edu.pl

but no papers have been devoted to the $5/7 = (A_2Cu_2O_3)_5(CuO_2)_7$ compounds. In the work of Abrashev et al. [10] there were presented the Raman spectra (for parallel polarizations) obtained for polycrystalline ceramics of the $Sr_{14}Cu_{24}O_{41}$-type structure. The authors concentrated on two-phonon and non-phonon spectral region (above 700 cm^{-1}) leaving the description of the results for one-phonon region (below 700 cm^{-1}) for the other paper, which, as far as we know, has not been published yet. Recently, two works on 7/10 crystals have been reported. In the first, magnetic excitations were investigated by the Raman scattering on single crystals of $Sr_{14-x-y}Ca_xY_yCu_{24}O_{41}$ [11] and in the second one the Raman measurements below 700 cm^{-1} have been performed on $Sr_{14-x}Ca_xCu_{24}O_{41}$ ($x = 0$ and 11.5) single crystals [12].

In the present paper we report the first results of Raman experiments on the single crystals of the $(Ca_{4.7}Sr_{4.1}Bi_{0.3})Cu_{17}O_{29}$ for all polarization configurations in backscattering geometry. Most measurements have been performed in the one-phonon region (from 40 to 700 cm^{-1}) in temperatures between 5 and 300 K. We also checked the existence of any features above 700 cm^{-1} in the whole temperature range. Finally, a possible peak assignment has been discussed.

2. Experimental

The investigated crystals of the $A_{10}Cu_{17}O_{29}$ ($A_{10} = Ca_{4.7}Sr_{4.1}Bi_{0.3}$) family were grown by the "melted band" method [13] using Bi_2CuO_4 as a flux. The chemical composition of the samples was determined by electron probe micro-analysis (EPMA). The crystal structure was studied [14] by the single crystal X-ray analysis and the high resolution transmission electron microscopy. Both methods indicated on the high quality of single crystals and proved the incommensurate chain/ladder structure of the investigated crystals. The compound is characterised by orthorhombic symmetry with the space group $F222$.

The Raman backscattering spectra were obtained using a micro-Raman setup containing a triple spectrometer (DILOR XY) with a liquid-nitrogen cooled CCD detector and an optical microscope. A 100× objective with a 0.95 numerical aperture was used to focus the incident laser beam on a spot of about 2 μm in diameter and to collect the light in the backscattering geometry. The spectral resolution was 1–2 cm^{-1}. The scattered light was excited by the 488 and 514.5 nm lines of an Ar^+ laser. The plasma lines were removed from the laser beam by using a small monochromator as a filter. To avoid overheating of the samples the output laser power was kept below 40 mW (at the sample surface it was about 100 times smaller). A continues flow Oxford Microstat was used for the experiment taken in the temperature range from 5 to 300 K. For low temperature measurement a 50× long distance (8 mm) objective lens with a 0.55 numerical aperture was used.

3. Results and discussion

In this study several crystals were tested with considerably good reproducibility. However, we observed little differences in the spectra from sample to

sample. We also noticed, like for other high-T_c superconductors, that the frequency of some peaks shifted to lower frequencies when laser beam power had increased too much (certainly because of laser beam heating). Sometimes rotational lines of N_2 and O_2 in ambient air interfered with the observation of Raman scattering from the samples below 100 cm^{-1}. However, since the positions of these rotational lines are well known, they were discriminated from the Raman spectra.

In order to analyze a complete set of polarized spectra obtained in definite conditions we performed the complete measurements on the same sample in the same conditions. The sample had the shape of elongated rectangular prism ($0.2 \times 0.3 \times 2.0$ mm^3) with the long dimension of the sample along the c-axis. The other two perpendicular edges were parallel to the a- and b-axes of the orthorhombic single crystal. The sample was irradiated through the 100× microscope objective with the 488 nm argon line and beam power of 20 mW at the laser exit. The same objective was used to collect the scattered light. Since some reflected light, especially at low frequencies, was also collected in our micro-Raman setup (more for parallel polarization than for crossed one), the spectra were measured in the range of 94–690 cm^{-1} for parallel configuration, while for configuration with crossed polarizations in the range of 42–646 cm^{-1}. The scale of the scattering intensities is given in photon counts detected in our CCD camera in a time period of 600 s. The spectra were not corrected for the sensitivity of the instrument in different scattering configurations.

The backscattering Raman spectra, obtained at the room temperature, in all possible polarization configurations, are shown in Figs. 1, 2, and 3 with the incident and scattered light vectors along a, b, and c axes, respectively. The polarizations are labelled according to the abbreviated Porto notation, where letters refer to the polarization of incident and scattered light, respectively. For example, yz in Fig. 1 is a shortening of $x(yz)\bar{x}$ (in the Porto notation) which indicates that the direction of incident beam light is parallel to the a-axis of the crystal with polarization parallel to the b axis and the scattered light is also parallel to the a-axis but in opposite direction with polarization along the c-axis. The y' and z' denotes the directions rotated by 45° with respect to the a and b axes around the c axis. For clarity the spectra were shifted in vertical scale of intensity and for comparison of the background scattering level in different configurations we gave the numbers at the left site of each spectrum showing the offset of the spectrum with respect to the zero of the absolute counts number in our experiment. The frequency values were controlled with the Ne lines. It was found that the peak position obtained from different measurements and different peak fittings were slightly different. Thus we evaluate the accuracy of the peak positions for about 3 cm^{-1}.

In Fig. 1 for zz spectrum there are peaks at 259 cm^{-1}, 299 cm^{-1} and very strong peak at 548 cm^{-1}. The spectra for $z'z'$ and $y'z'$ configurations are very similar. The first one is weaker than the zz spectrum and the second one is much stronger. There is also some shifting of the peak centres. The centre of the 259 cm^{-1} peak is shifted to the frequency of 255 cm^{-1} for $z'z'$ configuration, while the centre of the 299 cm^{-1} peak is shifted to higher frequency of 302 cm^{-1} for $y'z'$ configuration. For both configurations there is also some increase in frequency (about 2 cm^{-1}) of the major peak with respect to the zz configuration. Oppositely

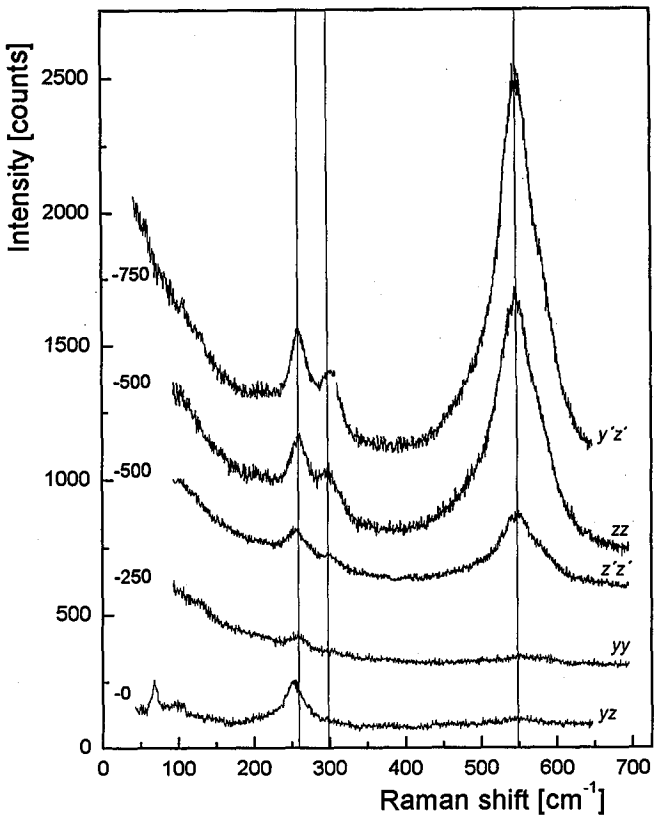

Fig. 1. Polarization dependent Raman spectra of $(Ca_{4.7}Sr_{4.1}Bi_{0.3})Cu_{17}O_{29}$ single crystal with incident and scattered light along the a-axis taken at room temperature. At the left site of each spectrum the numbers denote the zero-intensity level, at the right site the letters denote the polarization configuration. Vertical lines are for better comparison of the peak positions.

to the zz spectrum, for yy configuration practically there is no structure at all, just a very weak peak at about 257 cm^{-1}. For crossed polarizations yz we can see a radical change of the spectrum. There are only two peaks at 69 and 252 cm^{-1} and a very weak feature at around 100 cm^{-1}. It is worth to notice that the big difference between the yz and $y'z'$ spectra was obtained just with the rotation of the sample by 45° with respect to each other.

For configurations with the laser beam direction parallel to the b axis (Fig. 2) we can easily recognize the zz spectrum which is nearly identical with the analogous one in Fig. 1. In the spectrum xx the peaks at 259 cm^{-1} and 298 cm^{-1} are not present. In this region we can see only one peak at 313 cm^{-1}. There is again very strong structure for high frequency but now it is apparently composed of two peaks. The fitting with two Lorentz peaks gave the frequency values of 547 and 582 cm^{-1}. In the spectrum $x'x'$ we can see again the same double band with peaks at 547 and about 580 cm^{-1} as in the xx spectrum and some weak features between

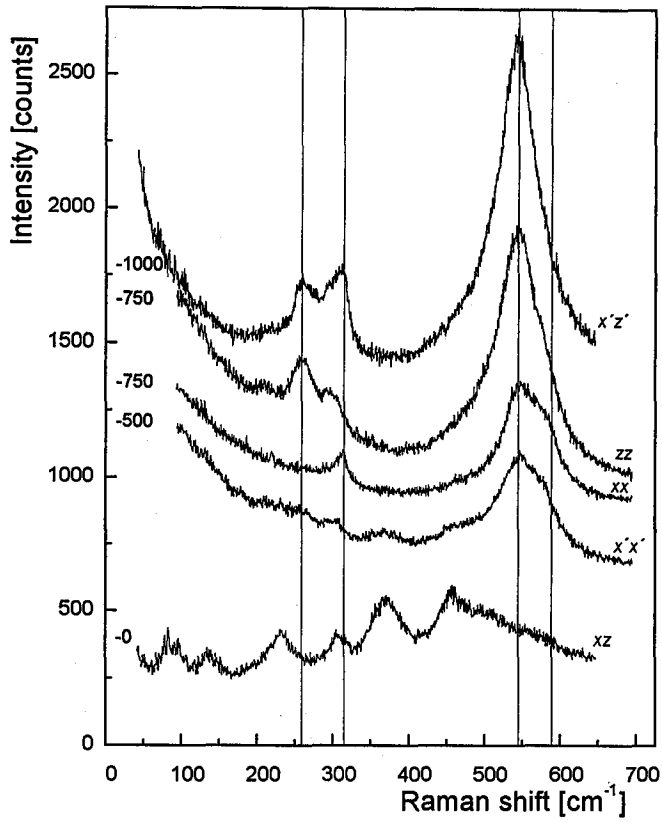

Fig. 2. Polarization dependent Raman spectra of $(Ca_{4.7}Sr_{4.1}Bi_{0.3})Cu_{17}O_{29}$ single crystal with incident and scattered light along the b-axis taken at room temperature. At the left site of each spectrum the numbers denote the zero-intensity level, at the right site the letters denote the polarization configuration.

200 and 400 cm^{-1}. For polarization $x'z'$ the lower energy peak in the double band strongly increased in intensity and shifted to lower values of about 544 cm^{-1}. The higher energy peak is not visible in this configuration. Except that dominating peak, we can see the peak at 259 cm^{-1} and stronger peak at 313 cm^{-1}. Probably there is still something at 299 cm^{-1} but it can be overshadowed by strong peak at 313 cm^{-1}.

The spectrum with crossed polarization xz is completely different from all other curves in the picture. There are peaks at 83, 97, 135, 232, 309, 372, and around 460 cm^{-1}. It should be mentioned that they are not present in other spectra, except (may be) the peak at 309 cm^{-1}. This rather complicated spectrum is not typical of high-T_c superconductors. However, because the crystal structure of the sample is very complicated, we can expect rather complicated spectra as well.

In Fig. 3 there are presented the spectra with the incident and scattered light along the c axis. The xx spectrum is the same as in Fig. 2, with slightly higher

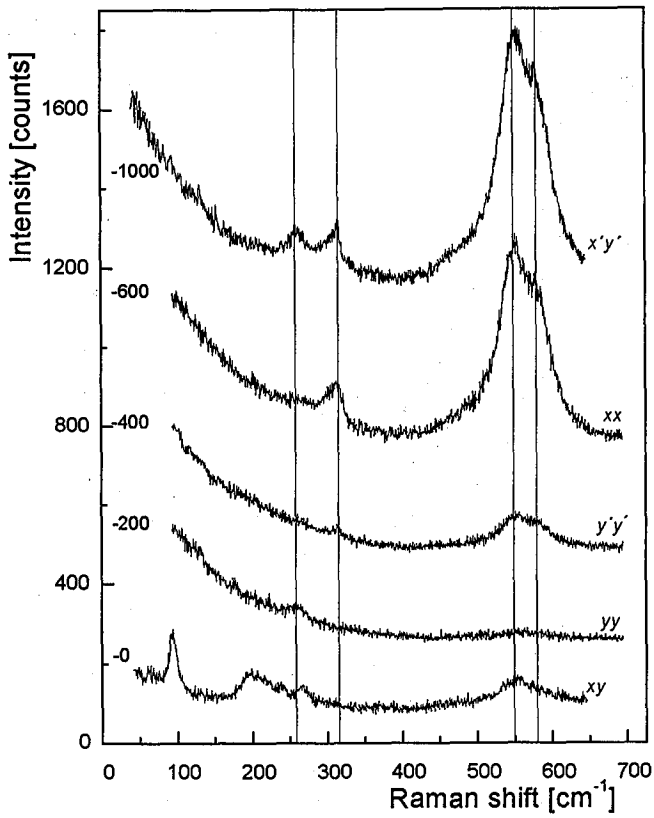

Fig. 3. Polarization dependent Raman spectra of $(Ca_{4.7}Sr_{4.1}Bi_{0.3})Cu_{17}O_{29}$ single crystal with incident and scattered light along the c-axis taken at room temperature. At the left site of each spectrum the numbers denote the zero-intensity level, at the right site the letters denote the polarization configuration.

values of the double peaks (550 and 584 cm^{-1}) and some smaller background at low frequencies. This is probably because in our micro-Raman setup less reflected light was collected from this surface, since the side surfaces of the as-grown crystals were metallic shiny, while the surfaces perpendicular to c axis were obtained by fracture. Again the yy spectrum is featureless. The $y'y'$ spectrum is very similar to the xx spectrum but simply weaker. For perpendicular polarizations along the diagonals $x'y'$ there are peaks at 259, 313, 550, and 585 cm^{-1}. The spectrum in crossed polarization xy has only one stronger peak at 94 cm^{-1}, much weaker bands at 200, 211, 236, 262, and a broad band at around 550 cm^{-1}, which may be a polarization leakage from other configuration.

The phonon spectra we observed for 5/7 crystal are in some respects similar to those reported in literature for 7/10 crystals [10–12]. Typical of both materials is the strong structure at around 545–585 cm^{-1} and a weaker one in the region of 250–300 cm^{-1}. The spectra with crossed polarizations are also to some extent similar. In contrast to 7/10 crystals we observed only very weak phonon scattering for yy configuration.

In our samples, otherwise than in [11], we do not see any magnon peaks. It is probably because in our superconducting samples magnetic correlations are completely suppressed. For the same reason we do not observe any peaks at frequencies higher than 700 cm^{-1} except very weak broad peak at around 1100 cm^{-1}, which well corresponds with two-phonon scattering frequency. In [10, 11] such peaks are designated as the one-magnon or two-magnon scattering peaks. It should be mentioned that the samples measured in [10, 11] are not superconducting ones therefore magnon peaks are to be observed.

The material under study has very attractive superconducting properties. Therefore, it is very interesting to check if there are any remarkable changes in Raman spectra in the vicinity of the transition temperature to the superconducting state. We did not notice big changes in the phonon scattering spectra in this temperature region. However, some changes have been observed in the electronic continuum seen as a featureless, almost flat, background. At temperatures $T < T_c$ the

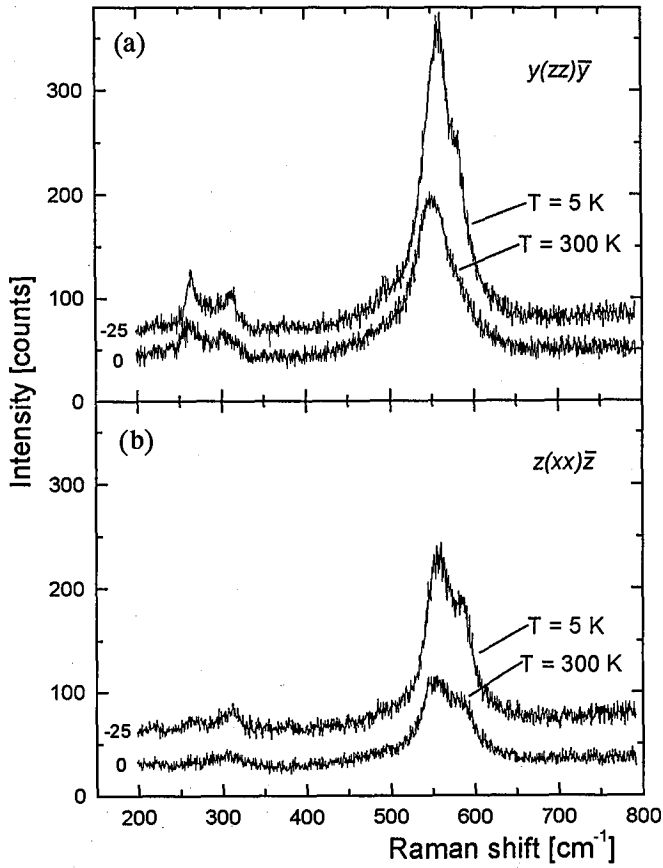

Fig. 4. The comparison of the Raman spectra in 5 and 300 K for (a) $y(zz)\overline{y}$ and (b) $z(xx)\overline{z}$ configurations. The spectra are shifted with respect to each other (the values are given at each spectrum).

electronic continuum displays a polarization dependent loss of scattering strength at low energies, since the electronic scattering with energy less than gap (2Δ) is suppressed by the opening gap. Therefore one should expect to observe a redistribution of the electronic continuum below T_c. Figures 4 and 5 show some examples of the Raman spectra changes when the temperature of the sample decreases to 5 K. Generally, we can see the increase in the intensity of nearly all peaks, their narrowing and frequency shift to higher values. In some spectra we could recognize new peaks. At $y(xz)\overline{y}$ spectrum we can notice the most pronounced changes with the temperature decreased to 5 K. The broad band at around 370 cm^{-1} is divided into two clear peaks at 363 and 385 cm^{-1}. There are also well visible peaks at 458, 483, 508, and broad band at around 560 cm^{-1}. Low energy peaks changed oppositely. They decreased with decreasing temperature. The different behaviour of these peaks can be connected with electronic scattering. Figures 4 and 5 display

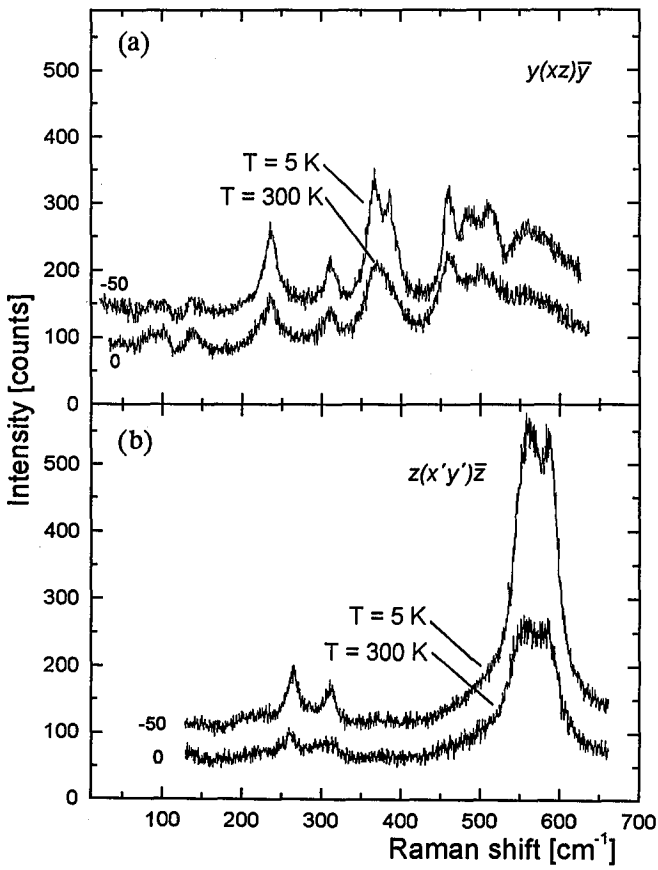

Fig. 5. The comparison of the Raman spectra in 5 and 300 K for (a) $y(xz)\overline{y}$ and (b) $z(x'y')\overline{z}$ configurations. The spectra are shifted with respect to each other (the values are given at each spectrum).

some interesting features which were not observed in 7/10 samples because they were studied only in the normal state. One can see clearly in Fig. 4 for configuration zz and xx as well as in Fig. 5 for configuration $x'y'$ the redistribution of the electronic continuum below approximately 320 cm^{-1}. This value is near the value of energy gap 2Δ ($\approx$ 300 cm^{-1}) determined in [6]. It confirms the intrinsic nature of superconductivity in 5/7 compounds. Because of the presence of phonon peaks the gap cannot be determined exactly and must be viewed as tentative and waiting confirmation in further experiments. The fact that the redistribution of the electronic continuum depends strongly on the polarization directions of light may be due to substantial gap anisotropy [6].

In Fig. 6 some peak positions as a function of temperature are shown in the range between 5 and 300 K. The positions do not show distinct changes during the decrease in temperature. With temperature going down to 5 K a typical shift (about 5 cm^{-1}) to higher frequencies was observed for most of the peaks. The exception was the peak at 548 cm^{-1}, which moved much stronger with temperature. For all the spectra a characteristic feature is a small shift of peak positions at 100 K i.e. near T_c.

The observed peaks are listed in Table with the values of Raman frequency, the polarization configurations at which they are visible, and the assigned modes in agreement with the orthorhombic structure. Peaks at 257, 300, 313, 547, and 582 cm^{-1} appear only in the spectra with parallel orientation of the polarization

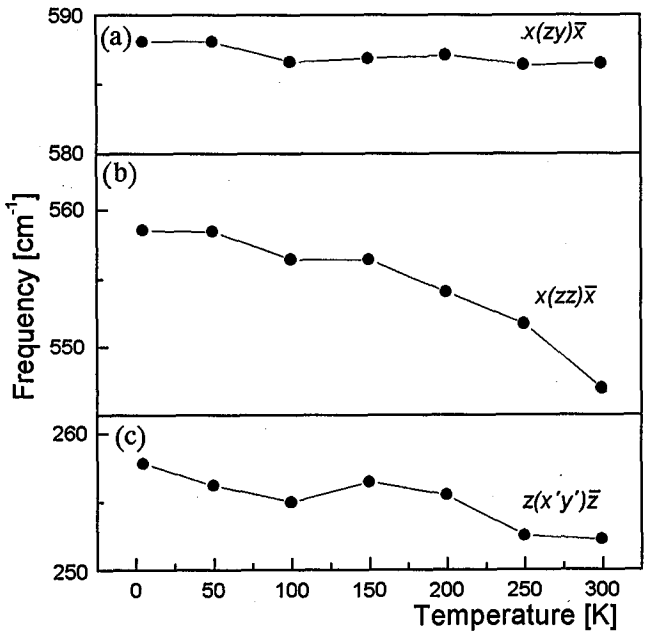

Fig. 6. The peak position dependence on temperature for (a) $x(zy)\overline{x}$, (b) $x(zz)\overline{x}$, and (c) $z(x'y')\overline{z}$ configurations.

TABLE

Experimental values of the Raman frequencies for $(Sr,Ca)_{10}Cu_{17}O_{29}$.

Frequency [cm^{-1}]	$x(--)\overline{x}$	$y(--)\overline{y}$	$z(--)\overline{z}$	Mode
69	yz			B_3
83		xz		B_2
94			xy	B_1
97		xz		B_2
135		xz		B_2
202			xy	B_1
211			xy	B_1
232		xz		B_2
236			xy	B_1
252	yz			B_3
255–259	$zz, yy, z'z', y'z'$	$zz, x'z'$	$yy, x'y'$	A
266			xy	B_1
298–302	$zz, z'z', y'z'$	zz		A
309		xz		B_2
313		$xx, x'z'$	$xx, x'y'$	A
363 (low temp)		xz		B_2
385 (low temp)		xz		B_2
458 (low temp)		xz		B_2
483 (low temp)		xz		B_2
508 (low temp)		xz		B_2
544–550	$zz, z'z', y'z'$	$zz, xx, x'x', x'z'$	$xx, x'x', xy, x'y'$	A
580–585		$xx, x'x'$	$xx, x'x', x'y'$	A

xx, yy, zz, $x'x'$, $z'z'$, and crossed configurations along diagonals (for example $x'z'$ or $y'z'$) but they are not visible for crossed xy, xz, or yz configurations. Therefore, these peaks correspond most probably to the A symmetry phonons in the orthorhombic structure. The rest of the peaks are visible only in crossed polarizations and they correspond to the B symmetry. The B modes are rather easy to identify, however, the A modes should be treated as proposition.

In Ref. [10] it is suggested that two high frequency A modes correspond to the "breathing" oxygen vibrations (along the x-direction) of the CuO_2 chains and Cu_2O_3 ladders. Because the 550 cm^{-1} peak is very sensitive to the temperature, we think that it can be connected with ladders, while the 580 cm^{-1} peak seems to be connected with chains. Further work should be done to make full assignment of all spectra peaks.

Acknowledgment

This work was partly supported by the Committee for Scientific Research under project 2 P03B 102 14.

References

[1] T. Siegrist, L.F. Schneemeyer, S.A. Sunshine, J.V. Waszczak, R.S. Roth, *Mater. Res. Bull.* **23,** 1429 (1988).

[2] E.M. Mccarron, M.A. Subramian, J.C. Calabrese, R.L. Harlow, *Mater. Res. Bull.* **23,** 1355 (1988).

[3] M. Matsuda, K. Katsumata, *Phys. Rev. B* **53,** 12201 (1996).

[4] H. Szymczak, R. Szymczak, M. Baran, L. Leonyuk, G.-J. Babonas, V. Maltsev, in: *New Development in High Temperature Superconductivity,* Eds. J. Klamut, B.W. Veal, B.M. Dąbrowski, P.W. Klamut, M. Kazimierski, Springer-Verlag, Berlin 2000, p. 157.

[5] R. Szymczak, H. Szymczak, M. Baran, E. Mosiniewicz-Szablewska, L. Leonyuk, G.-J. Babonas, V. Maltsev, L. Shvanskaya, *Physica C* **311,** 187 (1999).

[6] A.I. D'yachenko, V.Yu. Tarenkov, R. Szymczak, A.V. Abal'oshev, I.S. Abal'osheva, S.L. Lewandowski, L. Leonyuk, *Phys. Rev. B* **61,** 1500 (2000).

[7] M. Uehara, J. Akimitsu, H. Takahashi, N. Mori, K. Kinoshita, *J. Phys. Soc. Jpn.* **65,** 2764 (1996).

[8] M. Cardona, *Physica C* **317-318,** 30 (1999).

[9] M. Krantz, M. Cardona, *J. Low-Temp. Phys.* **99,** 205 (1995).

[10] M.V. Abrashev, C. Thomsen, M. Surtchev, *Physica C* **280,** 297 (1997).

[11] S. Sugai, M. Suzuki, *Phys. Status Solidi B* **215,** 653 (1999).

[12] N. Ogita, Y. Sakaguchi, Y. Fujino, T. Nagata, J. Akimitsu, M. Udagawa, *Physica B* **281&282,** 955 (2000).

[13] V. Maltsev, L. Leonyuk, G.-J. Babonas, R. Szymczak, A. Reza, *J. Cryst. Growth* **211,** 501 (2000).

[14] P. Dłużewski, A. Pietraszko, M. Kozłowski, A. Szczepańska, J. Górecka, M. Baran, L. Leonyuk, G.-J. Babonas, G. Van Tendeloo, O. Lebedev, R. Szymczak, *Acta Phys. Pol. A,* submitted for publication.